Available online at www.sciencedirect.com
ScienceDirect
Solid State Communications 143 (2007) 437–441
solid state communications
www.elsevier.com/locate/ssc

Rapid thermal annealing induced change of the mechanism of multiphonon resonant Raman scattering from ZnO nanorods

V.V. Ursaki[a,*], O.I. Lupan[b,c], L. Chow[c], I.M. Tiginyanu[a], V.V. Zalamai[a]

[a] *Laboratory of Low-Dimensional Semiconductor Structures, Institute of Applied Physics, Academy of Sciences of Moldova, Chisinau-2028, Republic of Moldova*
[b] *Department of Microelectronics and Semiconductor Devices, Technical University of Moldova, Chisinau-2004, Republic of Moldova*
[c] *Department of Physics, University of Central Florida, PO Box 162385 Orlando, FL 32816-2385, United States*

Received 5 April 2007; received in revised form 3 June 2007; accepted 4 June 2007 by D.J. Lockwood
Available online 12 June 2007

Abstract

Multiphonon Resonant Raman scattering (RRS) excited by 351.1 and 363.8 nm lines of an Ar^+ laser was studied at temperatures from 10 to 300 K in as-grown and rapid thermal annealed (RTA) aluminum doped ZnO nanorods synthesized by an aqueous chemical deposition method using zinc sulfate, aluminum sulfate, and ammonia hydroxide as precursors. RTA of ZnO nanorods at temperatures 650–750°C was found to result in changing the mechanism of RRS from incoming to outgoing. This change is suggested to be related to the RTA induced improvement of the optical properties of the nanorods.

PACS: 78.30.Fs; 78.55.Et; 81.05.Dz; 81.10.Dn

Keywords: A. Semiconductors; B. Chemical synthesis; E. Luminescence; E. Inelastic light scattering

1. Introduction

Nanosized semiconducting oxides have been focal points of great interest during the last ten years owing to their electrical and optical properties that are suitable for the fabrication of nanoscaled electronic and optoelectronic devices. Due to the multiple and switchable growth directions of Wurtzite structures and the high ionicity of polar surfaces [1], it assures conditions for the ZnO formation of a very rich micro/nanostructure diversity in comparison with other materials. Among ZnO nanostructures the arrays of nanorods attract special attention as microcavities for microlasers [2–4] owing to the large exciton binding energy in ZnO (60 meV) which ensures that excitonic emission is significant at room temperature. Apart from that, aluminum-doped zinc oxide (AZO) nanostructures are promising for nanoscopic research and various applications including gas sensors [5], solar cells [6], optical waveguide and exciton related devices [7]. One-dimensional ZnO nanorods with their high carrier mobility serve as direct conduction pathways for excitons.

Over the last ten years, different methods have been used to fabricate high-quality AZO thin films, such as RF thermal plasma evaporation, pulsed laser deposition, metalorganic chemical vapor deposition and sputtering, solution-liquid–solid growth in organic solvents, vapor–liquid–solid and vapor–solid processes. At the same time, the aqueous chemical deposition method became widely used for the fabrication of AZO nanostructures due to their economical and ecological advantages, low-temperature processing and the flexibility to tailor the properties by doping and modeling impurity distribution in the end product — nanorods and mesoporous films [8].

Resonant Raman scattering (RRS) has been proven to be an important tool for the study of basic physical properties of semiconductors, including nanostructured materials. It provides information pertaining to the electronic structure [9,10], electron–phonon coupling [11,12], radiation induced crystal damage [13], etc. However, one needs to take into account the mechanism of RRS when extracting this information. In this letter, we show that rapid thermal annealing (RTA) of

* Corresponding author. Tel.: +373 22 237508; fax: +373 22 319305.
E-mail address: ursaki@yahoo.com (V.V. Ursaki).

0038-1098/$ - see front matter © 2007 Elsevier Ltd. All rights reserved.
doi:10.1016/j.ssc.2007.06.001

ZnO nanorods produced by an aqueous chemical deposition method results in changing the RRS mechanism from incoming to outgoing which is related to the RTA induced improvement of optical properties of the nanorods.

2. Sample synthesis and experimental details

The template-free synthesis of the ZnO nanorods on Corning glass substrates was conducted by an aqueous-based solution route that involves hydrolysis, condensation and complexation reactions of metal salts using zinc sulfate, aluminum sulfate, and ammonia hydroxide as precursors. The ethylenediamine was also introduced in the precursor solution to make possible the growth process at low temperatures and to shorten the deposition time.

Before the growth process, the glass substrates were cleaned in a 20% HCl solution, rinsed in deionized water and ethanol:acetone (1:1) mixture, jet of deionized water and dried in a nitrogen flux. Subsequently, the substrates were sensitized in a $SnCl_2$/HCl solution and immersed horizontally in the precursor solution. The growth process was performed in an autoclave maintained at 85–95 °C for 20–40 min. After the hydrothermal reaction, the autoclave was cooled down to room temperature. The product was washed and dried at 200 °C for 10 min.

After the deposition process, the samples were subjected to rapid thermal annealing for 60 s at different temperatures ranging from 400 to 800 °C under low vacuum (10^{-1} Pa) conditions. The morphology and chemical composition microanalysis of samples were studied using a VEGA TESCAN TS 5130MM scanning electron microscope (SEM) equipped with an Oxford Instruments INCA energy dispersive X-ray (EDX) system. X-ray diffraction (XRD) analysis of the samples was performed with a Rigaku 'D/B max' X-ray diffractometer equipped with graphite monochromatized Cu K_α radiation ($\lambda = 1.54178$ Å) and optimized operating conditions of 30 mA and 40 kV at a scanning rate of 0.02°/s in the 2θ range of 10°–90°. The ultraviolet (UV) emission spectra were measured in backscattering geometry under excitation by 351.1 and 363.8 nm lines of an Ar^+ SpectraPhysics laser. The emission was analyzed by means of a double spectrometer having a resolution better than 0.5 meV. The samples were mounted on the cold station of a LTS-22-C-330 cryostat.

3. Morphology and structural characterization

The produced ZnO samples represent hexagonally shaped rods with the average diameter of 300–400 nm as deduced from the top SEM image illustrated in Fig. 1. The high quality of the grown ZnO rods is demonstrated by the stoichiometric composition deduced from the EDX analysis and by the XRD crystallographic data. Fig. 2 shows the XRD diffraction pattern of the ZnO nanorods. The diffraction peaks in the pattern are indexed to hexagonal Wurtzite structured ZnO (space group: $P6_3mc(186)$; $a = 0.3249$ nm, $c = 0.5206$ nm) and the data are in agreement with JCPDS card for ZnO (JCPDS 036-1451). The intensity of the peaks relative to the background signal

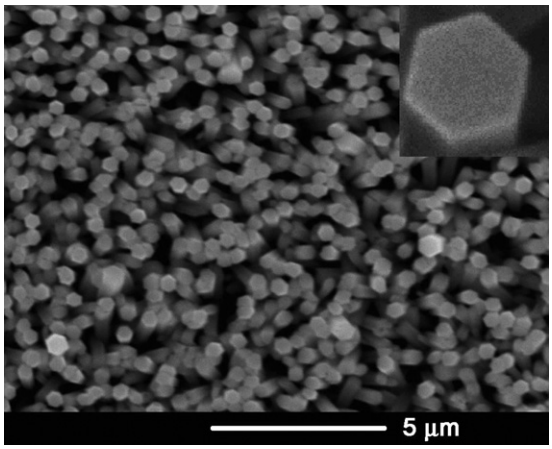

Fig. 1. Top view SEM image of ZnO nanorods grown on a glass substrate. Inserted is the image of an individual rod.

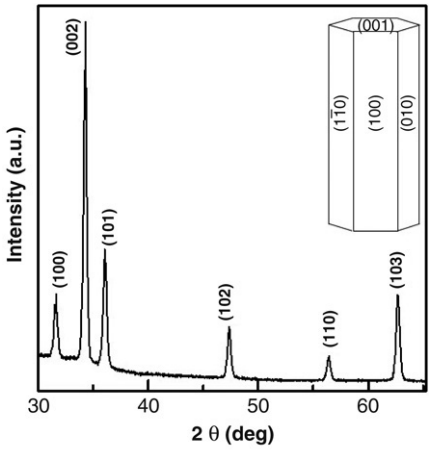

Fig. 2. XRD pattern of ZnO nanorods.

demonstrates the high purity of the ZnO hexagonal phase of the products and good crystallinity of the samples. The XRD pattern exhibits a (002) preferred orientation, which suggests that the rods are quasi-aligned with the optical C-axis oriented perpendicularly to the substrate surface. The texture coefficient for the (002) orientation is estimated to be about 2.7 from the following relation [14]:

$$TC_{(002)} = \frac{I_{(002)}/I^0_{(002)}}{(1/N)\sum I_{(hkl)}/I^0_{(hkl)}} \quad (1)$$

where N is the number of diffraction peaks, $I_{(hkl)}$ and $I^0_{(hkl)}$ are the measured and corresponding recorded intensities according to the JCPDS card, respectively. This value is comparable with the one inherent to the best ZnO nanorod samples [14].

4. Optical characterization

Fig. 3 illustrates the emission spectra of as-grown and RTA treated ZnO rods under excitation by the 351.1 nm laser line at 10 K. The spectrum of the as-grown sample consists of an

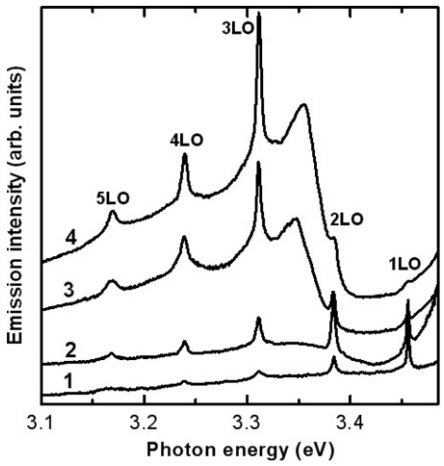

Fig. 3. Emission spectra of as-grown (1) and subjected to RTA (2–4) ZnO nanorods excited by 351.1 nm laser line at 10 K. The annealing temperature was 400 °C (2), 650 °C (3), and 750 °C (4).

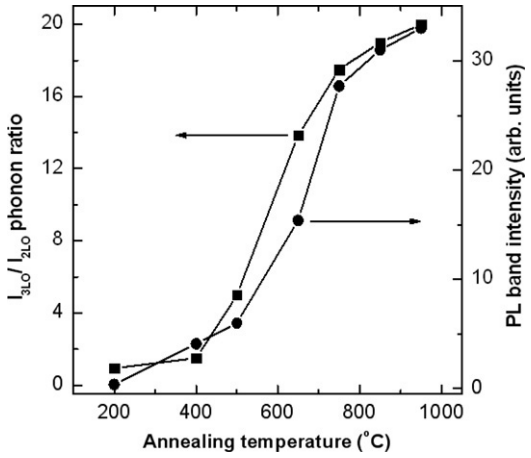

Fig. 4. The intensity ratio of 3LO to 2LO phonon lines in the resonant Raman scattering spectrum (squares, left-hand axis) and the intensity of the PL band (circles, right-hand axis) as a function of the annealing temperature. The samples were excited by a 351.1 nm laser line. Lines are an eye guide only.

RRS progression based on a fundamental 1LO band at 3.458 eV and its overtones. RRS from solids can be observed if the energy of the incoming or scattered photons matches the real electronic states in the material. This is referred to as incoming and outgoing resonance (see, e.g., Ref. [15]). The spectrum of the as-grown sample is typical for incoming RRS. The temperature dependence of the RRS spectrum of this sample as well as the analysis of RRS under excitation with different laser lines corroborates this suggestion. The shape of the spectrum is practically independent of the temperature as well as the energy of the excitation laser line. The temperature increase leads to the decrease of the RRS intensity and to the broadening of RRS peaks, while the ratio of the RRS lines intensity in the progression remains unchanged. In a hexagonal Wurtzite structure, the bands of polar modes are the superposition of A_1 and E_1 modes. Since the Raman scattering is performed with backscattering geometry, and according to XRD data the rods are aligned perpendicularly to the sample surface, the wave vectors of incident light $\boldsymbol{k}$ and that of collected scattered light $\boldsymbol{k'}$ are parallel to each other, and parallel to the C-axis of the rods. Therefore, the detected phonons with wave vector $\boldsymbol{q}$ propagate along the C-axis, implying that the main contribution to the RRS signal comes from the A_1 LO mode.

The RTA leads to a considerable modification of the emission spectrum. With the increase of the annealing temperature a broad and asymmetric PL line emerges on which the RRS lines are superimposed. Simultaneously, a redistribution of the RRS lines intensity occurs. It was previously shown [16,17] that in highly doped ZnO samples the PL band involved is mainly due to direct transitions of electrons between the conduction to valence band tails which are formed due to potential fluctuations induced by the high concentration of impurity according to the Morgan model [18]. It was also demonstrated that a clear correlation exists between the PL band and the RRS lines [17]. An analogous correlation between a near bandgap PL line and RRS was recently demonstrated in CdS nanowires [10]. The analysis of the RRS in RTA annealed samples as a function of temperature and excitation quantum energy indicates the

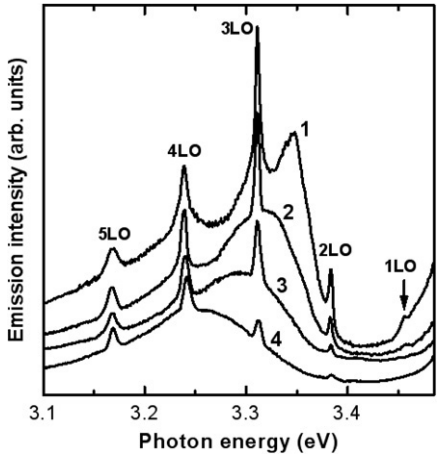

Fig. 5. Emission spectra of ZnO nanorods subjected to RTA at 650 °C. The sample was excited by a 351.1 nm laser line and the spectra were measured at 10 K (1), 150 K (2), 200 K (3), and 250 K (4).

outgoing regime of RRS in these samples where the energy of the outgoing photon resonates with electronic states in the impurity induced energy band tails. Fig. 4 presents the intensity ratio of 3LO to 2LO phonon lines in the resonant Raman scattering spectrum (I_{3LO}/I_{2LO}) as well as the intensity of the PL band as a function of annealing temperature. One can notice a clear correlation between the dependence of PL band intensity and I_{3LO}/I_{2LO} upon annealing temperature, similarly to the correlation between the I_{3LO}/I_{2LO} and free carrier concentration reported previously in ZnO samples with a high concentration of zinc interstitial defects [16,17]. We suggest that in the Al-doped rods subjected to RTA the potential fluctuations are induced by the activation of the Al impurity.

Figs. 5 and 6 show the emission spectra of ZnO rods annealed at 650 °C (Fig. 5) and at 750 °C (Fig. 6) measured at different temperatures from 10 to 300 K under the excitation by 351.1 nm (Fig. 5) and 363.8 nm (Fig. 6) laser lines. Fig. 7 presents the temperature dependence of the intensity ratio of 4LO to 3LO phonon lines along with the temperature

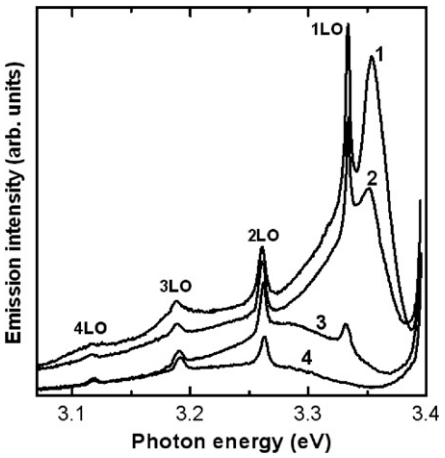

Fig. 6. Emission spectra of ZnO nanorods subjected to RTA at 750 °C. The sample was excited by a 363.8 nm laser line and the spectra were measured at 10 K (1), 100 K (2), 200 K (3), and 300 K (4).

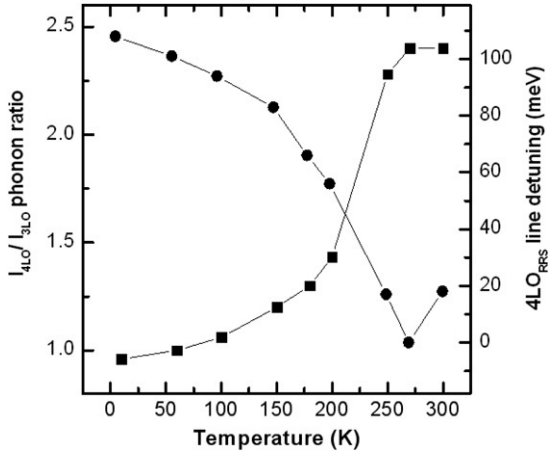

Fig. 7. Temperature dependence of the $4LO_{RRS}$ line detuning from the PL band position (circles, right-hand axis), and I_{4LO}/I_{3LO} phonon intensity ratio (squares, left-hand axis) measured under a 351.1 nm laser line excitation in ZnO rods annealed at 650 °C. Lines are an eye guide only.

dependence of the $4LO_{RRS}$ line detuning from the position of the PL band for ZnO rods annealed at 650 °C.

One can see that with increasing temperature the PL band shifts towards lower energies and broadens. At the same time, the temperature increase leads to the redistribution in the intensity of lines in the RRS in favor of the lines whose energy better matches the position of the luminescence band at a particular temperature. At low temperatures, the maximum of the PL band is closer to the energy of photons scattered by third-order LO phonons when excited by the 351.1 nm laser line, and to the energy of photons scattered by first-order LO phonons when excited by the 363.8 nm laser line. In accordance with the previous statement, the 3LO RRS line is more intense under the 351.1 nm laser line excitation, while the1LO RRS line dominates the RRS progression under the 363.8 nm laser line excitation. With the temperature increase, the PL band shifts towards the position of the 4LO overtone under the 351.1 nm laser line excitation, and towards the position of the 2LO overtone under the 363.8 nm laser line excitation. The spectra presented in Figs. 5 and 6 as well as the analysis in Fig. 7 clearly demonstrate the redistribution in favor of those RRS lines with increasing temperature.

We believe that the observed transition of RRS from the incoming to the outgoing mode with the increase of the RTA temperature and its relationship with the emerging PL band is due to the RTA induced improvement of the optical quality of ZnO rods. A decrease of the probability of non-radiative electronic transitions is expected to occur with an increase in the RTA temperature due to the thermal induced treatment of structural defects in the rods. The decrease of the density of structural defects leads to the redistribution of the recombination channels from non-radiative to radiative ones that results in the emerging of the PL band associated with electronic transitions from the conduction to the valence band tails. The intensity of this PL band increases with increasing the RTA temperature also due to the activation of the Al impurity.

Note in addition that the variation of the electron–phonon coupling may also influence the relative intensities of the members of the RRS progression in the LO phonon mode. It was recently shown that the coupling strength between electron and LO phonon diminishes with a decrease in the diameter of ZnO nanowires and quantum dots which results in the decrease of the second- to the first-order Raman scattering intensity [12,19,20]. However, we believe that the contribution from this mechanism is insignificant in our experiments. Firstly, we have not observed any significant change in the morphology of nanorods induced by RTA treatment. Apart from that, the diameter of the studied ZnO rods is too large significantly to affect the electron–phonon coupling.

5. Conclusions

The results of this study indicate the relevance of an eventual change in the mechanism of Resonant Raman Scattering when extracting from RRS experiments information related to physical processes occurring in bulk and nanostructured semiconductors materials. The RRS analysis in ZnO nanorods shows that apart from a previously demonstrated change of the RRS mechanism in ZnO structures induced by the variation of experimental conditions (temperature and excitation quantum energy) [17], technological processing may also lead to changing the RRS mechanism. In particular, RTA of AZO nanorods produced by a template free aqueous chemical deposition method on glass substrates results in changing the RRS mechanism from incoming to outgoing which is related to the RTA induced improvement of the optical properties of the nanorods.

Acknowledgments

This work was partly supported by the Science and Technology Center in Ukraine under Grant No. 4034 and by the Supreme Council for Research and Technological Development of the Academy of Sciences of Moldova. Oleg Lupan gratefully acknowledges the financial support from Moldovan Research and Development Association (MRDA) under funding from the US Civilian Research & Development Foundation (CRDF) under award no. MTFP-1014.

References

[1] P.X. Gao, Z.L. Wang, J. Appl. Phys. 97 (2005) 044304.
[2] M.H. Huang, S. Mao, H. Feick, H. Yan, Y. Wu, H. Kind, et al., Science 292 (2001) 1897.
[3] K. Govender, D.S. Boyle, P. O'Brien, D. Binks, D. West, D. Coleman, Adv. Mater. 14 (2002) 1221.
[4] T. Pauporte, D. Lincot, B. Viana, F. Pelle, Appl. Phys. Lett. 89 (2006) 233112.
[5] P. Mitra, H.S. Maiti, Sens. Actuators B 97 (2004) 49.
[6] D. Song, A.G. Aberle, J. Xia, Appl. Surf. Sci. 195 (2002) 291.
[7] S.D. Lester, F.A. Ponce, M.G. Craford, D.A. Steigerwald, Appl. Phys. Lett. 66 (1995) 1249.
[8] Lionel Vayssieres, Adv. Mater. 15 (2003) 464.
[9] D. Routkevitch, T.L. Haslett, L. Ryan, T. Bigioni, C. Douketis, M. Moskovits, Chem. Phys. 210 (1996) 343.
[10] A. Abdi, L.V. Titova, L.M. Smith, H.E. Jackson, J.M. Yarrison-Rise, J.L. Lensch, L.J. Lauhon, Appl. Phys. Lett. 88 (2006) 043118.
[11] A.P. Alivisatos, T.D. Harris, P.J. Carroll, M.L. Steigerwald, L.E. Brus, J. Chem. Phys. 90 (1989) 3463.
[12] H.-M. Cheng, K.-F. Lin, H.-C. Hsu, W.-F. Hsieh, Appl. Phys. Lett. 88 (2006) 261909.
[13] D. Pastor, J. Ibanez, R. Cusco, L. Artus, G. Gonzalez-Diaz, E. Calleja, Semicond. Sci. Technol. 22 (2007) 70.
[14] T. Mahalingam, K.M. Lee, K.H. Park, S. Lee, Y. Ahn, J.-Y. Park, K.H. Koh, Nanotechnology 18 (2007) 035606.
[15] P.Y. Yu, M. Cardona, Fundamentals of Semiconductors, Springer-Verlag, Berlin, Heidelberg, New York, 1996.
[16] V.V. Zalamai, V.V. Ursaki, E. Rusu, P. Arabadji, I.M. Tiginyanu, L. Sirbu, Appl. Phys. Lett. 84 (2004) 5168.
[17] V.V. Ursaki, I.M. Tiginyanu, V.V. Zalamai, E.V. Rusu, G.A. Emelchenko, V.M. Masalov, E.N. Samarov, Phys. Rev. B 70 (2004) 155204.
[18] T.N. Morgan, Phys. Rev. 139 (1965) A343.
[19] R.P. Wang, G. Xu, P. Jin, Phys. Rev. B 69 (2004) 113303.
[20] H.-M. Cheng, K.-F. Lin, H.-C. Hsu, C.-J. Lin, L.-J. Lin, W.-F. Hsieh, J. Phys. Chem. B 109 (39) (2005) 18385.